



Hyperspectral SAR

January 7, 2016

Matt Ferrara

Andrew Homan

Margaret Cheney

Matrix Research

Dayton, Ohio

Distribution A

PA# 88ABW-2016-0016

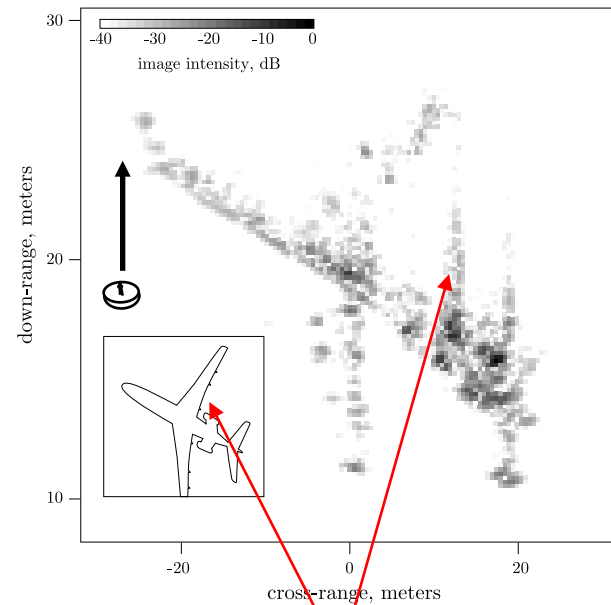


- Problem definition & related work
- Physical model & imaging algorithm
- Point spread function (PSF)-based resolution analysis
- Circular SAR example using Xpatch data
- Conclusions

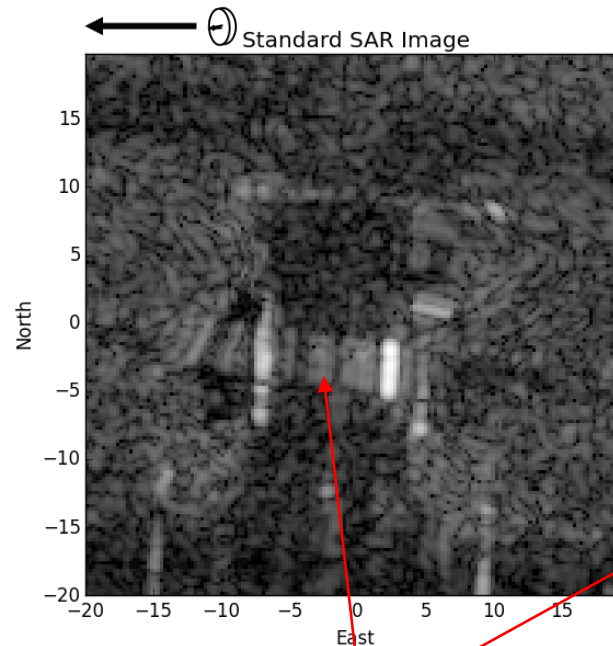


Problem

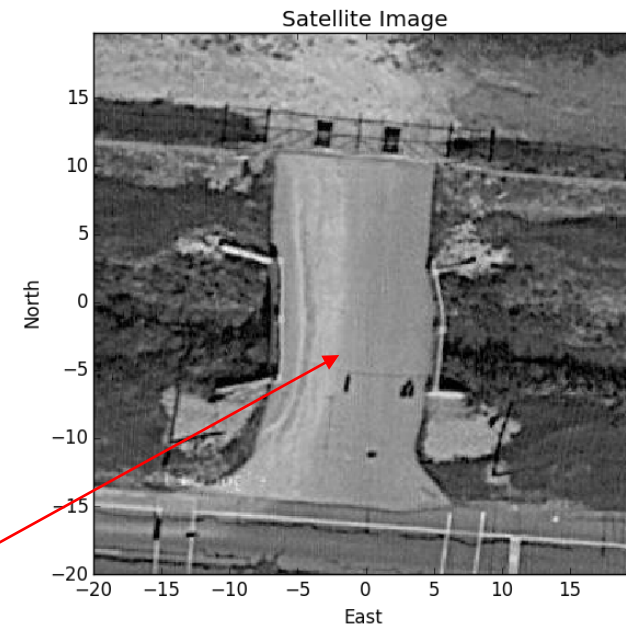
- Typical SAR imaging techniques neglect dispersion in scene reflectivity
- Below are examples of inadequately modeled structural dispersion



streaks above the engine inlets



streak across bridge span





- Waveform and geometry specific
 - Chirps → de-chirped phase history data
 - Zak-space estimation (Tolimieri). Used start-stop approximation.
 - *We wanted a method which was not restricted to a specific waveform or flight geometry*
- Parametric dispersion models
 - Extract simple parametric models from distortions in standard SAR (Gilman & Tsynkov) and ISAR (Borden) images
 - *We wanted to avoid restrictions to parametric models*
- Frequency-domain-based processing
 - Sub-banding (Albanese & Medina), frequency-domain filters (e.g., Garren 2002)
 - Frequency-domain pixel representations may have non-zero negative-time coefficients
 - *These methods do not explicitly enforce a causal model for dispersion*



- Scalar wave propagation from antenna to scene

$$\left(\nabla^2 - \frac{1}{c^2} \frac{\partial^2}{\partial t^2} \right) \mathcal{E}(t, \mathbf{x}) = s(t, \mathbf{x})$$

- Time-dependent reflectivity model

$$\mathcal{E}^{tot} = \mathcal{E}^{in} + \mathcal{E}^{sc}$$

$$s = s^{in} + s^{sc} \leftarrow \text{Models scattering object}$$

Models transmit antenna \rightarrow

$$s^{sc}(t, \mathbf{x}) = - \int_{t-\Delta T}^t v(t-t', \mathbf{x}) \mathcal{E}^{tot}(t', \mathbf{x}) dt'$$

\rightarrow supported on $0 \leq t-t' \leq \Delta T$

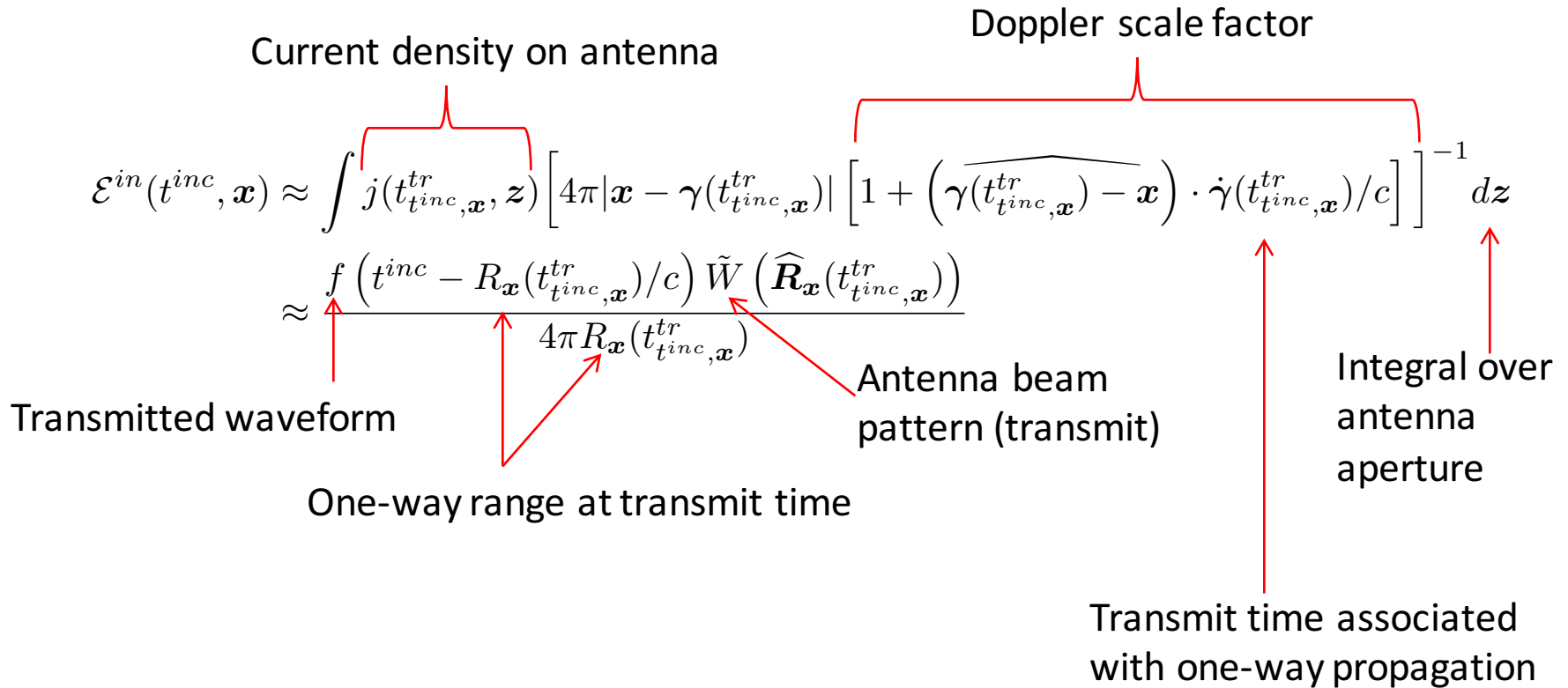
- “Standard” SAR uses $v(t-t', \mathbf{x}) = v(\mathbf{x})\delta(t-t')$



Incident Field Model

$$s^{in}(t, \mathbf{x} - \boldsymbol{\gamma}(t)) = -j(t, \mathbf{x} - \boldsymbol{\gamma}(t))$$

$$\mathcal{E}^{in}(t^{inc}, \mathbf{x}) = \int g(t^{inc} - t', \mathbf{x} - \mathbf{y}) j(t', \mathbf{y} - \boldsymbol{\gamma}(t')) dt' d\mathbf{y}$$





- Lippmann-Schwinger equation

$$\begin{aligned}\mathcal{E}^{sc}(t, \mathbf{x}) &= - \int \int g(t - \tau, \mathbf{x} - \mathbf{z}) s^{sc}(\tau, \mathbf{z}) d\tau d\mathbf{z} \\ &= \int \int g(t - \tau, \mathbf{x} - \mathbf{z}) \int \left(v(\tau - t', \mathbf{z}) \mathcal{E}^{tot}(t', \mathbf{z}) \right) dt' d\tau d\mathbf{z}\end{aligned}$$

where $g(t, \mathbf{x}) = \frac{\delta(t - |\mathbf{x}|/c)}{4\pi|\mathbf{x}|} = \int \frac{e^{i\omega(t - |\mathbf{x}|/c)}}{8\pi^2|\mathbf{x}|} d\omega$

- Born-approximated Lippmann-Schwinger equation

replace \mathcal{E}^{tot} with \mathcal{E}^{in}

$$\begin{aligned}\mathcal{E}_B^{sc}(t, \mathbf{x}) &= \iint g(t - t^{rad}, \mathbf{x} - \mathbf{y}) \underbrace{\int_0^{\Delta T} v(\Delta\tau, \mathbf{y}) \mathcal{E}^{in}(t^{rad} - \Delta\tau, \mathbf{y}) d\Delta\tau}_{s_B^{sc}(t^{rad}, \mathbf{y})} dt^{rad} d\mathbf{y} \\ &= \int \frac{\delta(t - t^{rad} - |\mathbf{x} - \mathbf{y}|/c)}{4\pi|\mathbf{x} - \mathbf{y}|} s_B^{sc}(t^{rad}, \mathbf{y}) dt^{rad} d\mathbf{y}\end{aligned}$$



- Weighted matched filter

$$I(\Delta\tau, \mathbf{z}) = \int \frac{R_{\mathbf{z}}(t^{rec}) R_{\mathbf{z}}(t_{t^{rec}, \Delta\tau, \mathbf{z}}^{tr}) f^*(t_{t^{rec}, \Delta\tau, \mathbf{z}}^{tr}) \chi_{\Delta\tau, \mathbf{z}}(t^{rec})}{\tilde{A}(\widehat{\mathbf{R}}_{\mathbf{z}}(t^{rec})) \tilde{W}(\widehat{\mathbf{R}}_{\mathbf{z}}(t_{t^{rec}, \Delta\tau, \mathbf{z}}^{tr}))} d(t^{rec}) dt^{rec}$$

Receive beam pattern
Transmit beam pattern
Measured data

Cutoff function

- Round-trip travel time $t^{rec} - t_{t^{rec}, \Delta\tau, \mathbf{z}}^{tr} = \frac{R_{\mathbf{z}}(t^{rec})}{c} + \Delta\tau + \frac{R_{\mathbf{z}}(t_{t^{rec}, \Delta\tau, \mathbf{z}}^{tr})}{c}$

- Resulting point spread function (PSF)

$$I(\Delta\tau, \mathbf{z}) = \int_{\Omega_{\mathbf{z}}} \int_0^{\Delta T} K(\Delta\tau, \mathbf{z}, \Delta\sigma, \mathbf{y}) v(\Delta\sigma, \mathbf{y}) d\Delta\sigma d\mathbf{y}$$

$$K(\Delta\tau, \mathbf{z}, \Delta\sigma, \mathbf{y}) = \int_{\Delta T_{\Delta\tau, \mathbf{z}}^{rec}} \left(\frac{R_{\mathbf{z}}(t^{rec}) R_{\mathbf{z}}(t_{t^{rec}, \Delta\tau, \mathbf{z}}^{tr})}{R_{\mathbf{y}}(t^{rec}) R_{\mathbf{y}}(t_{t^{rec}, \Delta\sigma, \mathbf{y}}^{tr})} \frac{\tilde{W}(\widehat{\mathbf{R}}_{\mathbf{y}}(t_{t^{rec}, \Delta\sigma, \mathbf{y}}^{tr})) \tilde{A}(\widehat{\mathbf{R}}_{\mathbf{y}}(t^{rec}))}{\tilde{W}(\widehat{\mathbf{R}}_{\mathbf{z}}(t_{t^{rec}, \Delta\tau, \mathbf{z}}^{tr})) \tilde{A}(\widehat{\mathbf{R}}_{\mathbf{z}}(t^{rec}))} \right) f^*(t_{t^{rec}, \Delta\tau, \mathbf{z}}^{tr}) f(t_{t^{rec}, \Delta\sigma, \mathbf{y}}^{tr}) dt^{rec}$$

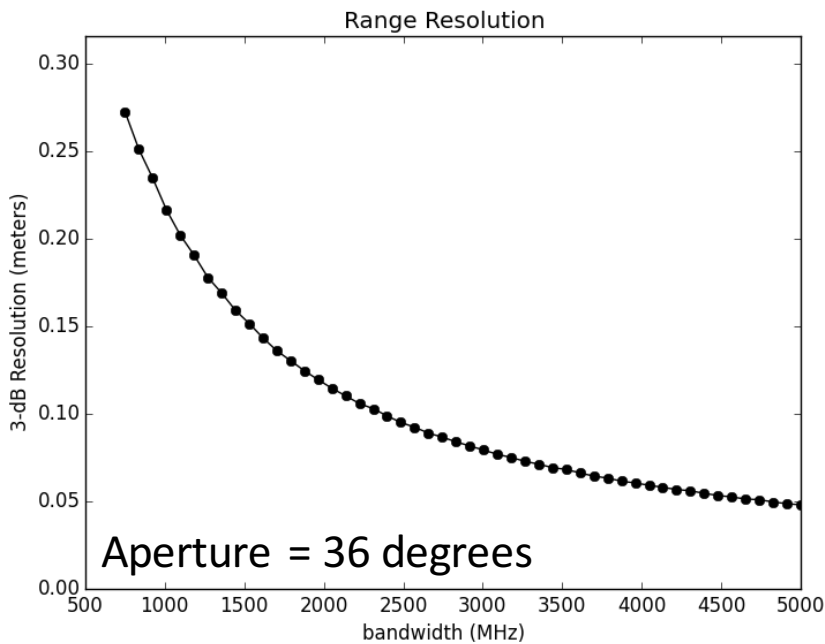


Range Resolution: 3-dB Main Lobe

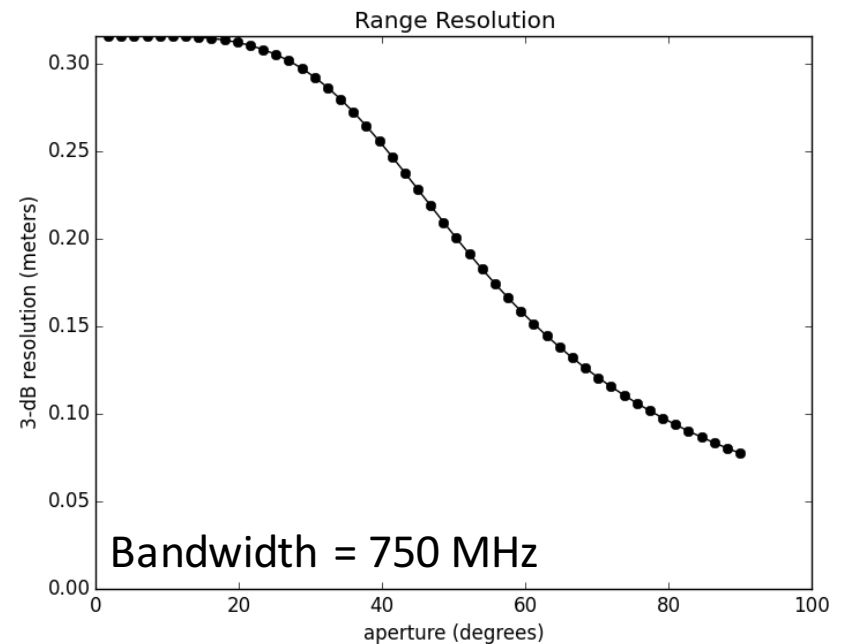


- Circular SAR example, 40-degree elevation
- Chirp time-bandwidth product = 100

Fixed Aperture + Increasing Bandwidth



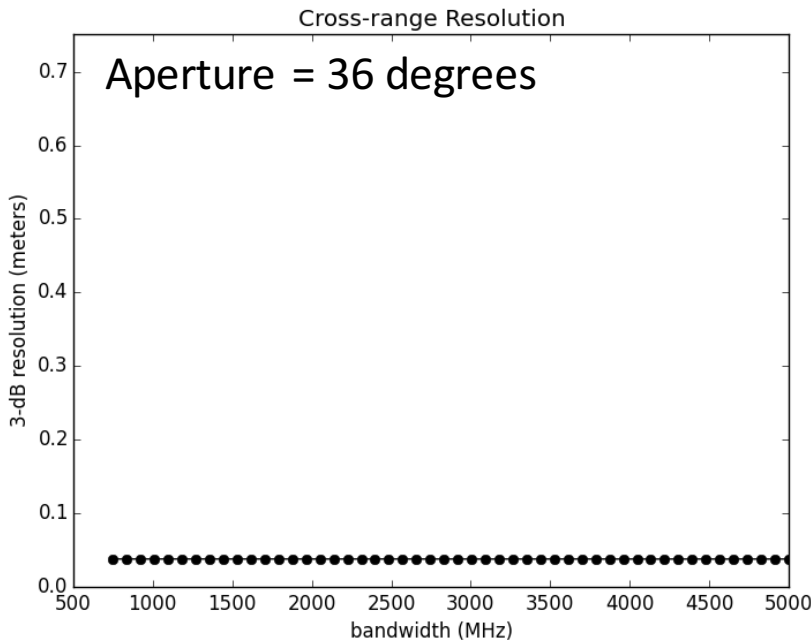
Increasing Aperture + Fixed Bandwidth



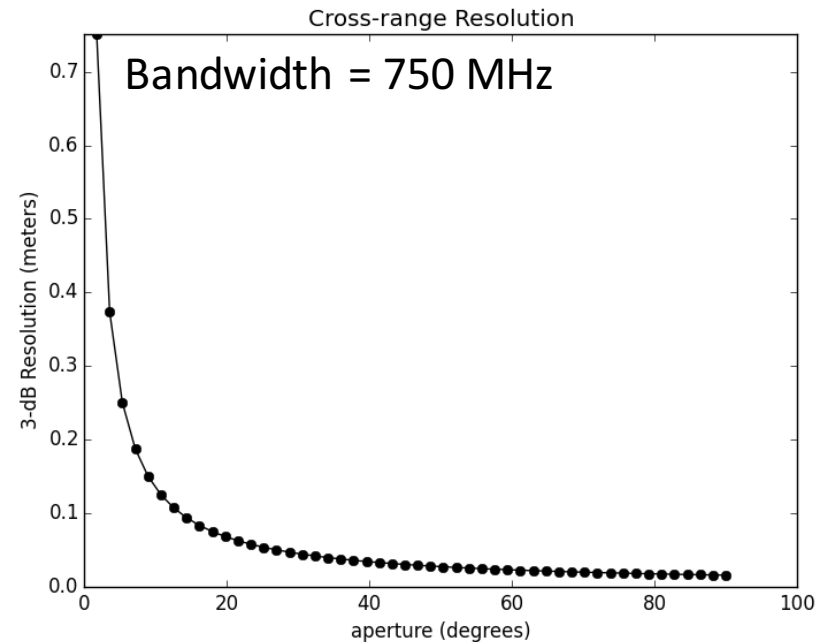


- Circular SAR example, 40-degree elevation
- Chirp time-bandwidth product = 100

Fixed Aperture + Increasing Bandwidth



Increasing Aperture + Fixed Bandwidth

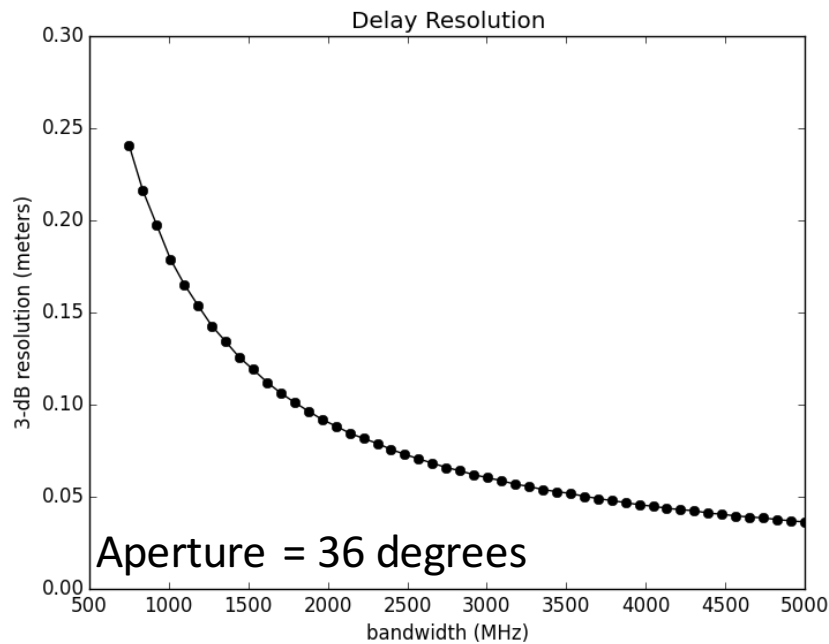




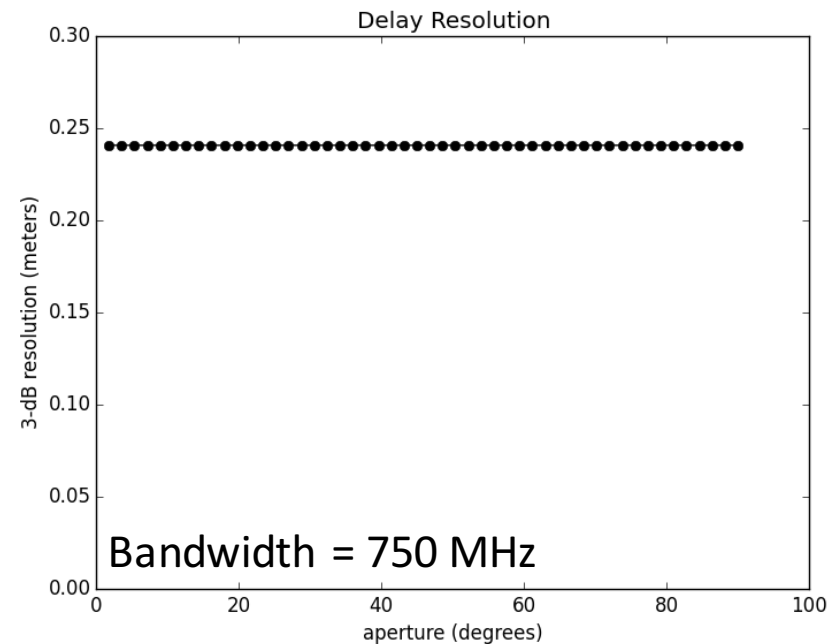
Delay Resolution: 3-dB Main Lobe

- Circular SAR example, 40-degree elevation
- Chirp time-bandwidth product = 100

Fixed Aperture + Increasing Bandwidth



Increasing Aperture + Fixed Bandwidth

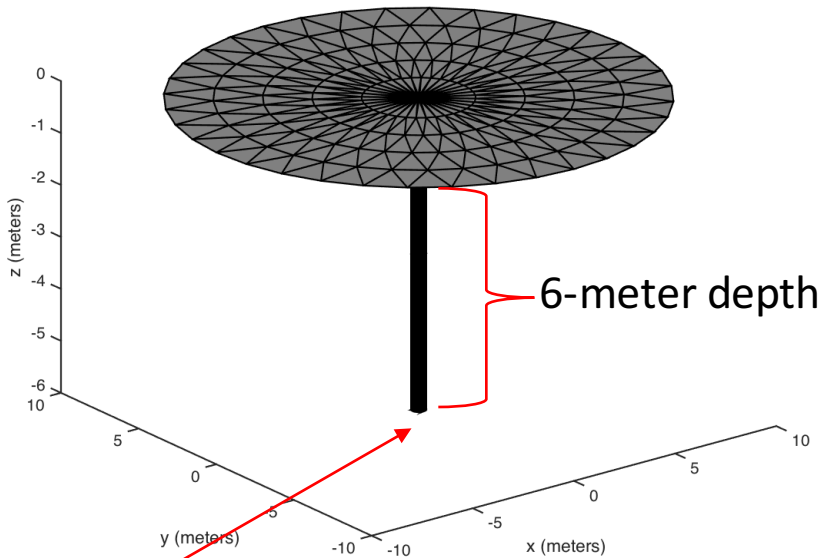




CSAR example: “bottom hat”

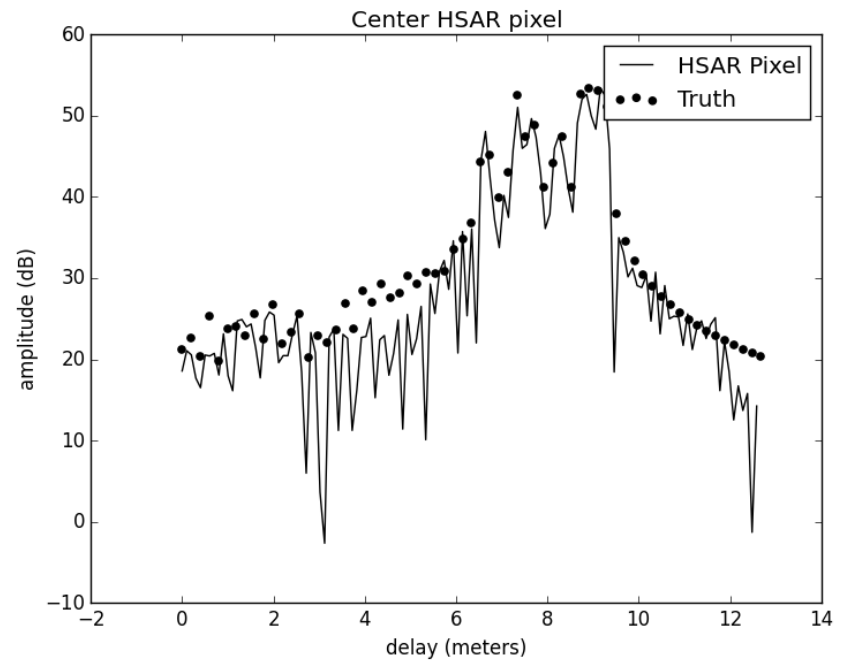
- Circular SAR with 36-degree aperture, 40-degree elevation angle
- 190 km flight-path radius, 69 m/s velocity
- Tukey-windowed 745 MHz chirp. $T \cdot BW = 100$. Center frequency = 10 GHz

Closed-end Cylinder Target



0.3-meter cylinder radius

Truth Vs. Reconstructed Reflectivity

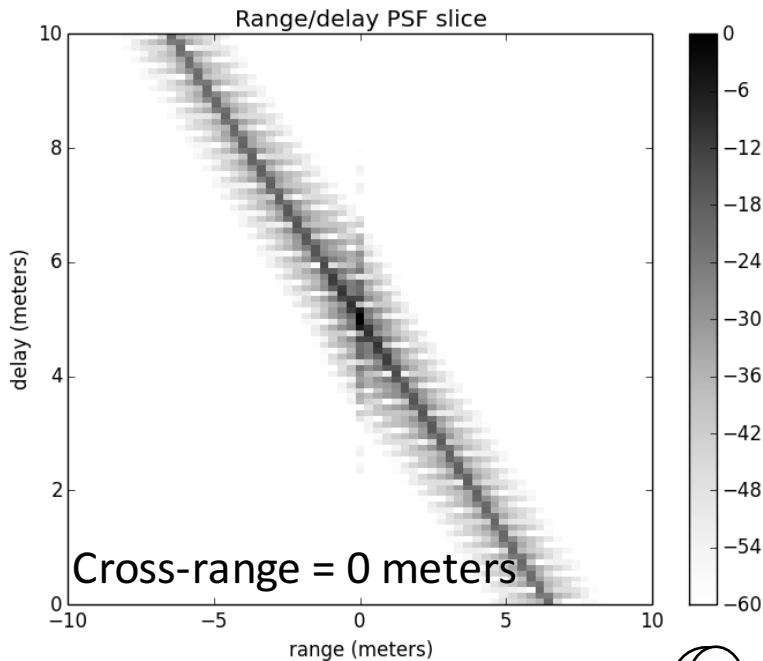




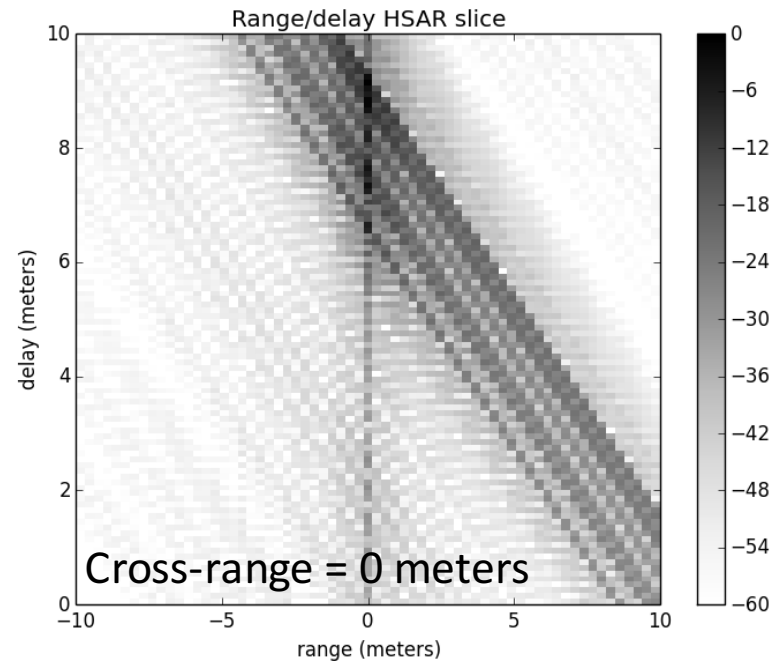
CSAR example: “bottom hat”

- Circular SAR with 36-degree aperture, 40-degree elevation angle
- 190 km flight-path radius, 69 m/s velocity
- Tukey-windowed 745 MHz chirp. $T \cdot BW = 100$. Center frequency = 10 GHz

Point Spread Function
Delay Vs. Range



HSAR Image
Delay Vs. Range

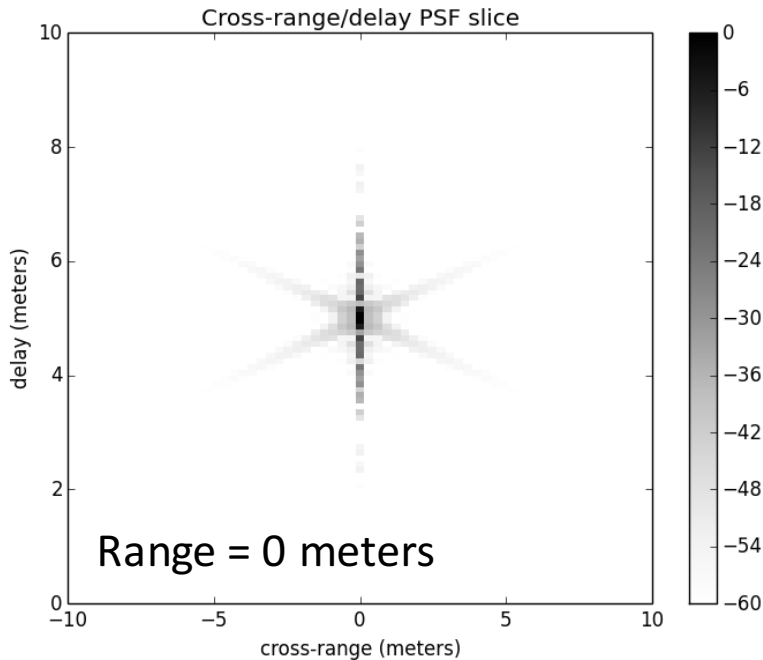




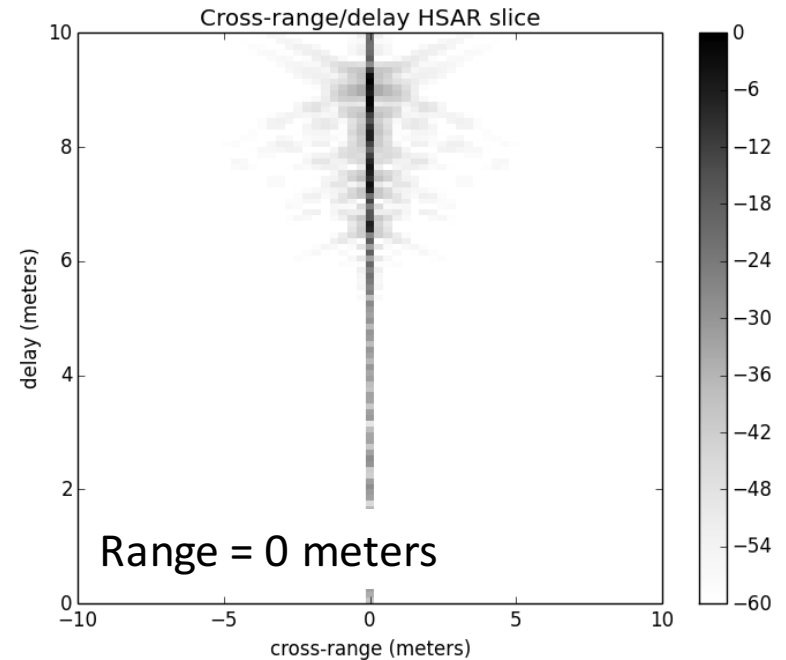
CSAR example: “bottom hat”

- Circular SAR with 36-degree aperture, 40-degree elevation angle
- 190 km flight-path radius, 69 m/s velocity
- Tukey-windowed 745 MHz chirp. $T \cdot BW = 100$. Center frequency = 10 GHz

Point Spread Function
Delay Vs. Cross Range



HSAR Image
Delay Vs. Cross Range

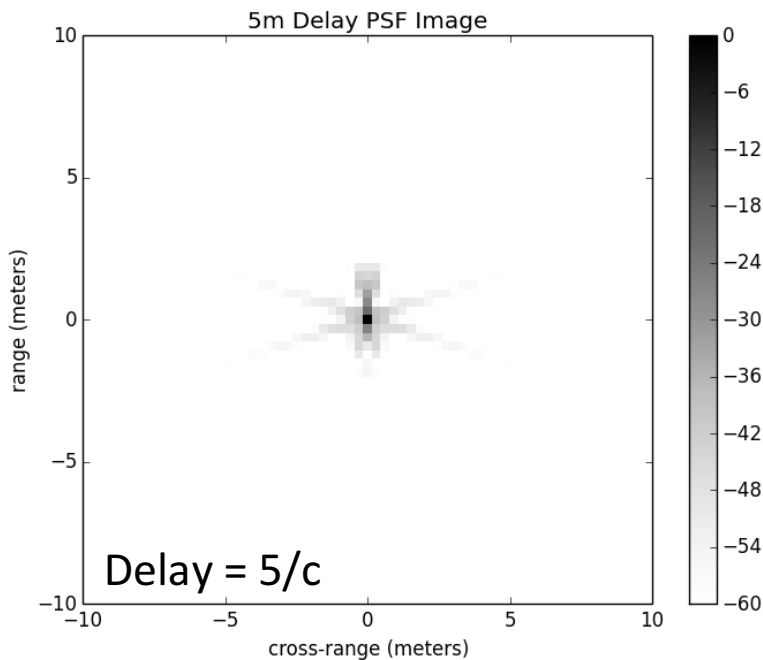




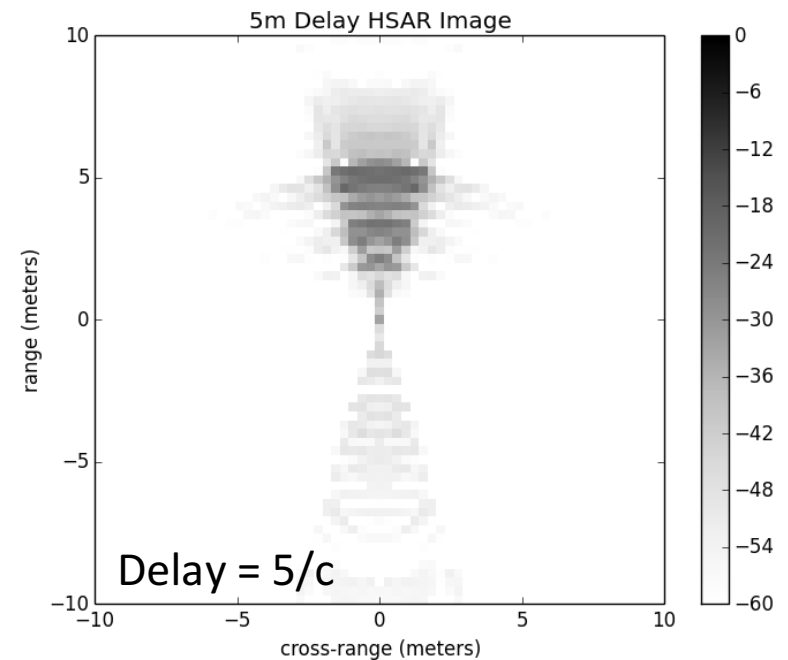
CSAR example: “bottom hat”

- Circular SAR with 36-degree aperture, 40-degree elevation angle
- 190 km flight-path radius, 69 m/s velocity
- Tukey-windowed 745 MHz chirp. $T \cdot BW = 100$. Center frequency = 10 GHz

Point Spread Function
Range Vs. Cross Range



HSAR Image
Range Vs. Cross Range

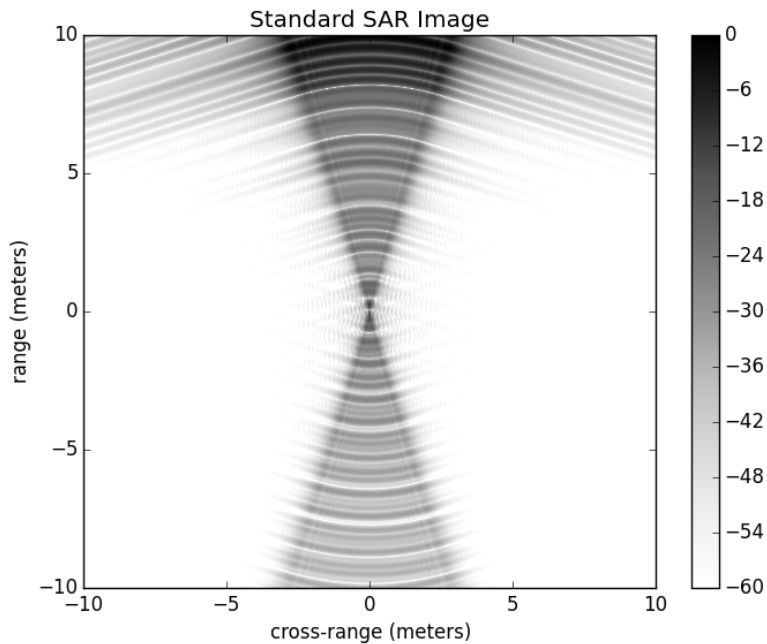




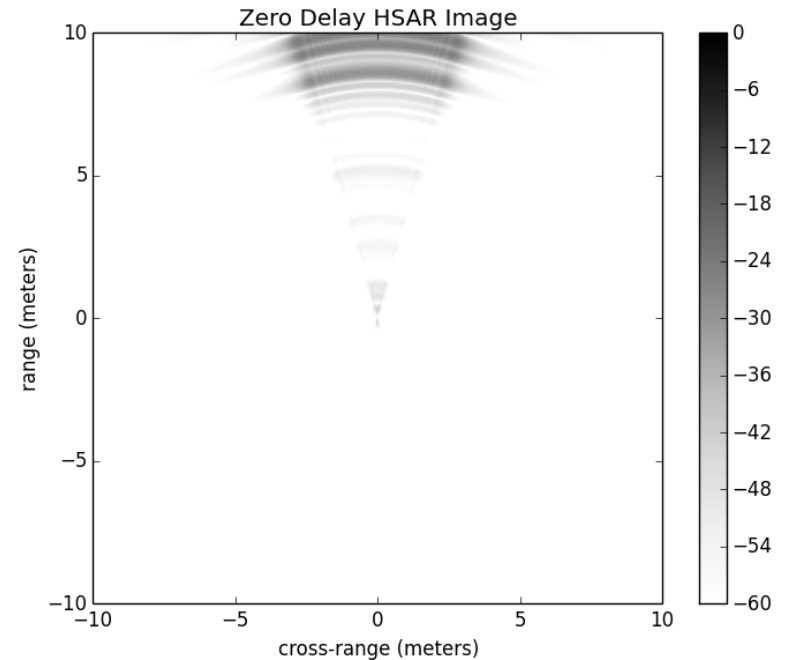
CSAR example: “bottom hat”

- Circular SAR with 36-degree aperture, 40-degree elevation angle
- 190 km flight-path radius, 69 m/s velocity
- Tukey-windowed 745 MHz chirp. $T^*BW = 100$. Center frequency = 10 GHz

Start-stop + Matched Filter + NUFFT



HSAR Image, $\Delta\tau = 0$





- We have developed and analyzed a time-domain algorithm for HSAR which
 - accommodates *arbitrary transmit strategies*
 - naturally restricts scene-reflectivity estimates to *causal* functions
- Point spread function (PSF)-based resolution analysis indicates
 - When BW and aperture are varied independently we see the following enhancements in resolution:

	BW	Aperture
Range	✓	✓
Cross Range	✗	✓
Delay	✓	✗

- Based on our experiments with Xpatch-generated data, it is possible to reconstruct structural dispersion parameters provided *sufficient bandwidth* and *aperture* (as predicted by the PSF)